

# Automatic Pseudorotaxane Formation Targeting on Nucleic Acids Using a Pair of Reactive Oligodeoxynucleotides

Kazumitsu Onizuka,<sup>\*,†,‡</sup> Fumi Nagatsugi,<sup>‡</sup> Yoshihiro Ito,<sup>†</sup> and Hiroshi Abe<sup>\*,†,§,||</sup>

<sup>†</sup>Nano Medical Engineering Laboratory, RIKEN, 2-1, Hirosawa, Wako, Saitama 351-0198, Japan

<sup>‡</sup>Institute of Multidisciplinary Research for Advanced Materials, Tohoku University, 2-1-1 Katahira, Aoba-ku, Sendai, Miyagi 980-8577, Japan

<sup>§</sup>Faculty of Pharmaceutical Sciences, Hokkaido University, Kita-12, Nishi-6, Kita-ku, Sapporo 060-0812, Japan

<sup>||</sup>PRESTO, Japan Science and Technology Agency, 4-1-8, Honcho, Kawaguchi-Shi, Saitama 332-0012, Japan

## S Supporting Information

**ABSTRACT:** Here we report a novel method to form a pseudorotaxane architecture using only a pair of reactive oligodeoxyribonucleotides (ODNs), which we designed and synthesized, and then performed the pseudorotaxane formation reaction with both DNA and RNA oligonucleotides. The reaction proceeded smoothly without any extra reagents at 37 °C and pH 7.2, leading to the formation of a stable complex on a denaturing polyacrylamide gel. Interestingly, the pseudorotaxane was formed with the cyclized ODN reversibly by the slipping process. This new pseudorotaxane formation represents a promising method for developing new DNA nanotechnologies and antisense oligonucleotides.

Rotaxane is a multicomponent structure consisting of a dumbbell shaped molecule and a macrocycle. The macrocycle is threaded onto the axle of the dumbbell, and the molecular architecture cannot be separated without bond cleavage. In supermolecular chemistry, rotaxanes have been studied for use as molecular machines, including molecular motors and molecular shuttles.<sup>1,2</sup> Recently, the property of a rotaxane-based molecule was expanded to the synthesis of small peptides<sup>3</sup> and unique catalysts.<sup>4–7</sup> In nucleic acid chemistry, topological molecular architectures, such as rotaxanes and catenanes, have been studied for DNA nanotechnology,<sup>8–13</sup> topological labels,<sup>14–17</sup> and the stabilization of triplex formation.<sup>18–20</sup> Generally, these were constructed enzymatically, but a variety of chemical methods to construct such architectures have been developed to expand the application. For example, Seeman et al. used the coupling reaction between an amino group and a carboxy group across a helical turn for catenane formation.<sup>17</sup> Additionally, DNA template-directed photoligation with 5-vinyl-2'-deoxyuridine derivatives gave some reversibly interlocked structures.<sup>20,21</sup> However, these methods require external stimuli such as a chemical reagent or light irradiation to form topological structures. A method that requires no external stimuli should be ideal for expanding this molecular architecture in physiological conditions. The formation of interlocked architectures in physiological conditions is an attractive approach, and should lead to a variety of applications, including new DNA nanotechnologies and antisense oligonucleotides.<sup>22</sup> In this paper, we

report a novel chemical reaction for automatic pseudorotaxane formation that targets nucleic acids using a pair of reactive oligodeoxyribonucleotides (ODNs). Here, we assumed that a pair of reactive ODNs prefer the template reaction at a suitably low concentration to provide the desired product.

We designed a pair of reactive ODNs. One contains a dibenzylcyclooctyne (DBCO) group at the internal position and a phosphorothioate group at the 3'-end. The other ODN contains an azide group at the internal position and a chloroacetyl group at the 5'-end. The S<sub>N</sub>2 type chemical ligation reaction between phosphorothioate and chloroacetyl groups proceeds only when two oligos hybridize with DNA or RNA at the same time at the proper position.<sup>23</sup> Copper-free click chemistry<sup>24–26</sup> between DBCO and azide was expected to occur across a helical turn. The two chemical reactions induced by hybridization with target nucleic acids should lead to the formation of a pseudorotaxane architecture (Figure 1).

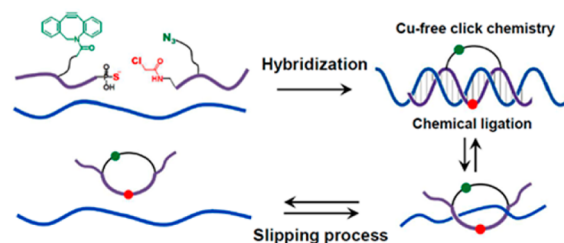


Figure 1. Schematic representation of pseudorotaxane formation.

All ODN and ORN sequences used are shown in Table 1, and the modified structures are shown in Figure 2. The pitch of a helix in a B-form DNA–DNA complex and an A-form DNA–RNA complex is 10 and 11 base pairs, respectively.<sup>27</sup> We expected that, to make a threaded structure for pseudorotaxane, a distance of >10 base pairs was required between DBCO and the azide group.<sup>17</sup> In addition, a longer, moderately flexible linker for the reactive group required for click chemistry would facilitate an efficient reaction.

ODN1 (X = T, DBCO) and 2 (X = T, DBCO) were synthesized by reacting ODN1 (X = T, NH<sub>2</sub>) and 2 (X = T,

Received: February 21, 2014

Published: May 7, 2014

Table 1. ODN and ORN Sequences Used in This Paper

entry	sequences (5'-3')
ODN1	(FAM)-TTGCGTXGCGC-S (X = T, R <sup>1</sup> )
ODN2	TTGCGTXGCGC-S (X = T, R <sup>1</sup> )
ODN3	ZCACYGCCCGC (Y = T, R <sup>2</sup> , Z = T, R <sup>3</sup> )
ODN4	FAM-AAAGCGGGCAGTGAGCGCAACGCAATTA
ODN5	TAGGGTXGGCA-S (X = T, R <sup>1</sup> )
ODN6	TAGGGTXGGCA-S (X = T, R <sup>1</sup> )
ODN7	ZCAGYAGCGCA (Y = C, R <sup>2</sup> , Z = C, R <sup>3</sup> )
ODN8	FAM-AAAGTGGCTGCTGGTGCCAACCCTATTGT
ODN9	GTTCAXCGGCGT-S (X = C, R <sup>1</sup> )
ODN10	ZCATYGTCCGG (Y = C, R <sup>2</sup> , Z = T, R <sup>3</sup> )
ODN11	FAM-CTTCCCGACGATGACGCCGGTGAACCTC
ODN12	TTGCGTTGCGTCACTGCCCGC
ORN1	FAM-AAAGCGGGCAGUGAGCGCAACGCAAUUA
ORN2	FAM-AAAGUGCGCUGCUGUGCCAACCCUAUUGU
ORN3	FAM-CUUCGGACGAUGACGCCGGUGAACUUC

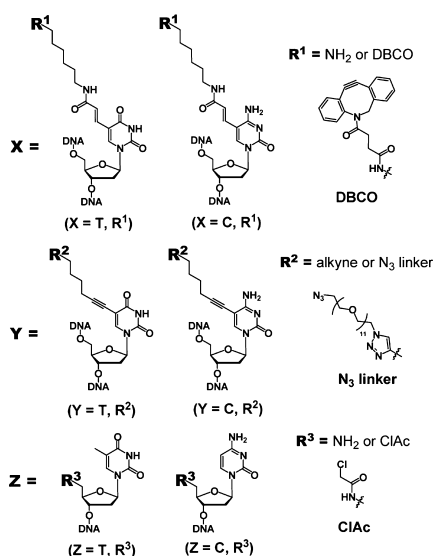
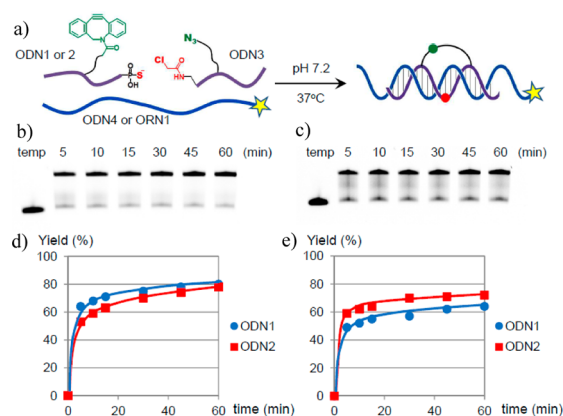


Figure 2. Structure of modified nucleosides.

NH<sub>2</sub>) and the DBCO NHS ester under alkaline conditions in high yields (Figure S1). ODN3 (Y = T, N<sub>3</sub> linker, Z = T, ClAc) was prepared from ODN3 (Y = T, alkyne, Z = T, NH<sub>2</sub>) by click chemistry and the coupling with chloroacetyl NHS ester (Figure S2). These ODNs were purified by reversed-phase HPLC and characterized by MALDI-TOF MS (Table S1).

Initially, each chemical ligation and copper-free click chemistry reaction was tested to check the reaction efficiency. Chemical ligation between phosphorothioate and the chloroacetyl group with either a DNA or RNA template proceeded rapidly at 37 °C and pH 7.2 to give the ligated product with a yield >80% within 5 min. In contrast, no reaction occurred without the template (Figure S3). This high efficiency and selectivity of the reaction are eligible for the hybridization-induced reaction. In contrast, Cu-free click chemistry proceeded relatively slowly over 1 h to give product yields of 49% and 47% when DNA and RNA templates were used, respectively. Nonetheless, the reaction was much faster than the reaction without the template (Figure S4).

The pseudorotaxane formation reaction was carried out with ODN1 (X = T, DBCO) or 2 (X = T, DBCO), ODN3 (Y = T, N<sub>3</sub> linker, Z = T, ClAc), and template ODN4 or ORN1 at 37 °C and pH 7.2 (Figure 3) and analyzed by denaturing PAGE analysis (Figure 3b,c). The reactions proceeded efficiently to give a new



**Figure 3.** Pseudorotaxane formation reactions. The reaction was carried out with a pair of reactive ODNs (2 μM) and template ODN or ORN (1 μM) in phosphate buffer (20 mM, pH 7.2) containing NaCl (150 mM), MgCl<sub>2</sub> (20 mM), and DTT (1 mM) at 37 °C. (a) Schematic representation of pseudorotaxane formation. (b) PAGE analysis of DNA-templated reaction using ODN1 (X = T, DBCO), ODN3 (Y = T, N<sub>3</sub> linker, Z = T, ClAc), and ODN4. (c) PAGE analysis of RNA-templated reaction using ODN2 (X = T, DBCO), ODN3 (Y = T, N<sub>3</sub> linker, Z = T, ClAc), and ORN1. (d) Time-dependent DNA-templated reaction using ODN1 or 2, ODN3, and ODN4. (e) Time-dependent RNA-templated reaction using ODN1 or 2, ODN3, and ORN1.

band in about 80% transformation for DNA and about 70% transformation for RNA within 1 h (Figure 3b–e). The reaction efficiency was higher than that for the copper-free click chemistry with non-ClAc-modified ODN3 (Figure S4), suggesting that the first formation of the ligated strand accelerated the click chemistry by an intramolecular reaction. The resulting complexes were extracted from gels and analyzed by MALDI-TOF MS measurements. Two peaks were observed: one corresponding to the template and the other was cyclized ODN (Figure S5). These results support the formation of pseudorotaxane structures, although the peak of the complex was not observed. In the reaction with nonazide-modified ODN3 (Y = T, alkyne, Z = T, ClAc), the band of the complex was absent, because no linkage across a helical turn was formed. However, the band of the duplex was observed, especially when the RNA template was used (Figure S6). Also, no bands of the complex were seen when a mismatch sequence was used (Figure S6). In the DNA template reaction, ODN1 showed a more efficient reaction than ODN2 (Figure 3d). In contrast, ODN2 was better than ODN1 when the RNA template was used (Figure 3e). Since the position of modified nucleosides is important for the effective proximity between DBCO and azide, the linkers should link more efficiently for both DNA–DNA and DNA–RNA duplexes because the distance fits the helical turn.<sup>27</sup> For the optimization of the reaction, the lengths of the DBCO linker were changed (Figure S7). The reaction with the C6 linker was as efficient as the reaction with the original C4 linker. In contrast, the reaction with the PEG linker was less efficient and gave a lower yield. Furthermore, the pseudorotaxane formation reaction was studied in detail to confirm the generality (Figure S8). We tested two different sequences of DNA or RNA template (ODN8 and ODN11 as the DNA template, and ORN2 and ORN3 as the RNA template) and ran the reaction using three pairs of reactive ODNs (Table 1). Pseudorotaxane formation was observed for all combinations, and the efficiency was similar to that for ODN1–ODN3 and ODN2–ODN3 pairs. These results indicate that this

pseudorotaxane formation reaction proceeds efficiently with sequence-selectivity and generality.

Next, to verify the formation of the threaded structures, the catenane formation was attempted with M13mp18 DNA (7,249 bases) as the template. This DNA is a single-stranded circular type. The reaction was carried out with ODN1 ( $X = T$ , DBCO, 5'-FAM) and ODN3 ( $Y = T$ ,  $N_3$  linker,  $Z = T$ , ClAc), which have complementary sequences toward M13mp18 DNA. The reaction was analyzed by HPLC after 2.5 h, and a new peak with the fluorescence of FAM (Ex: 494 nm, Em: 521 nm, blue line) appeared in 75% yield (Figure 4a). The product was stable

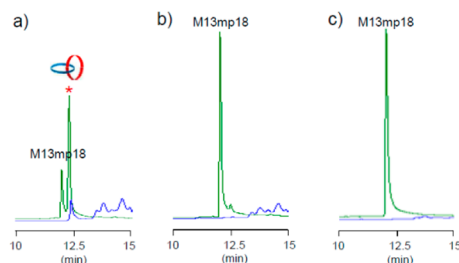


**Figure 4.** Catenane formation reactions. The reaction was carried out with a pair of reactive ODNs ( $1 \mu\text{M}$ ) and M13mp18 DNA ( $0.1 \mu\text{M}$ ) in phosphate buffer (20 mM, pH 7.2) containing NaCl (150 mM),  $\text{MgCl}_2$  (20 mM), and DTT (1 mM) at  $37^\circ\text{C}$  for 2.5 h. (a) M13mp18 DNA + ODN1 ( $X = T$ , DBCO, 5'-FAM) + ODN3 ( $Y = T$ ,  $N_3$  linker,  $Z = T$ , ClAc). New peak (\*) was observed. (b) ODN1 ( $X = T$ , DBCO, 5'-FAM) + ODN3 ( $Y = T$ , alkyne,  $Z = T$ , ClAc). (c) M13mp18 DNA only. Green line: detection by UV (260 nm). Blue line: detection by fluorescence (Ex: 494 nm, Em: 521 nm).

to heating at  $90^\circ\text{C}$  for 10 min. The peak was not observed in the reaction with nonazide-modified ODN3 ( $Y = T$ , alkyne,  $Z = T$ , ClAc) (Figure 4b). These results indicate that the new peak is the catenated DNA, which is also supported by the formation of catenane observed by Seeman's group.<sup>17</sup> These results suggest that our reactive ODNs form threaded structures with template DNA or RNA.

The thermodynamic stability of the pseudorotaxane was investigated by denaturing PAGE analysis. The isolated complex was heated in the absence of metal cations at pH 7.2 for 10 min and quenched by loading buffer and rapid cooling to  $0^\circ\text{C}$ . The results of the PAGE analysis and the ratio of pseudorotaxane are shown in Figure 5. The ratio of pseudorotaxane sharply decreased after heating at  $70^\circ\text{C}$  for both DNA–DNA and DNA–RNA pseudorotaxanes. The  $T_m$  values were measured with normal duplexes of ODN12–ODN4 and ODN12–ORN1 to compare the thermodynamic stability with the pseudorotaxane in the absence of metal cations at pH 7.2. The  $T_m$  value was  $64^\circ\text{C}$  for the ODN12–ODN4 duplex and  $66^\circ\text{C}$  for the ODN12–ORN1 duplex. Given that pseudorotaxane disassembled at  $60$ – $70^\circ\text{C}$ , these results indicate that pseudorotaxane formation does not stabilize the duplex thermodynamically. Next, we compared the stability of pseudorotaxane with a normal duplex on a denaturing polyacrylamide gel. ODN12–ODN4 and ODN12–ORN1 duplexes were not observed on the denaturing polyacrylamide gel containing 30% formamide. In contrast, the bands of pseudorotaxanes were observed (Figure 6). The threaded architecture is more stable than the canonical architecture under conditions that weaken H-bond forces. The stability against athermal denaturation is a unique property of the pseudorotaxane, and unlike the canonical short duplex.

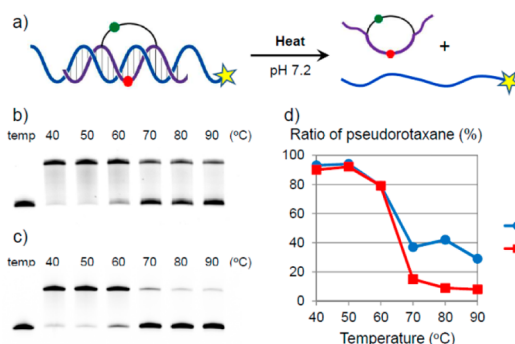


**Figure 5.** Stability of pseudorotaxane. The disassembly was carried out with pseudorotaxane ( $1 \mu\text{M}$ ) in Tris-HCl buffer (50 mM, pH 7.2) by heating at  $40$ – $90^\circ\text{C}$  for 10 min, and then rapidly cooling to  $0^\circ\text{C}$ . (a) Schematic representation of pseudorotaxane disassembly. (b) PAGE analysis of DNA–DNA pseudorotaxane (ODN1–ODN3–ODN4) disassembly. (c) PAGE analysis of DNA–RNA pseudorotaxane (ODN2–ODN3–ORN1) disassembly. (d) The ratio of pseudorotaxane after heating.

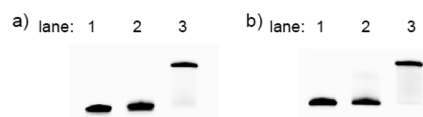


**Figure 6.** Comparison of the stability of pseudorotaxane with that of a normal duplex on denaturing polyacrylamide gel containing 30% formamide. (a) Lane 1, ODN4; lane 2, normal duplex (ODN12–ODN4); lane 3, DNA–DNA pseudorotaxane (ODN1–ODN3–ODN4). (b) Lane 1, ORN1; lane 2, normal duplex (ODN12–ORN1); lane 3, DNA–RNA pseudorotaxane (ODN2–ODN3–ORN1).

In Figure 5, DNA–DNA pseudorotaxane was present to  $\sim 30\%$ , even after heating at  $90^\circ\text{C}$ . We hypothesized that during cooling the cyclized ODN reformed pseudorotaxane with the template by the slipping process cooling to  $0^\circ\text{C}$  (Figure 7).<sup>19,28</sup> The cyclized ODN was synthesized from ODN1 ( $X = T$ , DBCO) or ODN2 ( $X = T$ , DBCO) and the highly reactive iodoacetyl-modified ODN3 ( $Y = T$ ,  $N_3$  linker,  $Z = T$ , IAc) in highly

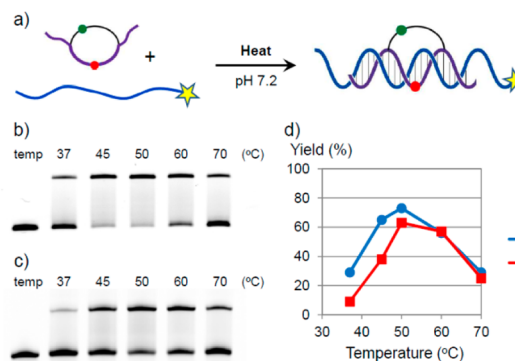


**Figure 7.** Pseudorotaxane formation by the slipping process. The formation was carried out with cyclized ODN ( $1.5 \mu\text{M}$ ) and template ( $1.0 \mu\text{M}$ ) in Tris-HCl buffer (50 mM, pH 7.2) by heating at  $37$ – $70^\circ\text{C}$  for 10 min, and then rapidly cooling to  $0^\circ\text{C}$ . (a) Schematic representation of the pseudorotaxane formation by slipping process. (b) PAGE analysis of DNA–DNA pseudorotaxane (ODN1–ODN3–ODN4) formation. (c) PAGE analysis of DNA–RNA pseudorotaxane (ODN2–ODN3–ORN1) formation. (d) The yield of pseudorotaxanes after heating.

concentrated solutions without a template. The pseudorotaxane formation reaction by the slipping process was carried out with cyclized ODN and the template by heating for 10 min and then rapidly cooling to 0 °C. The band of pseudorotaxane was observed, and the efficiency peaked at 50 °C in reactions involving both DNA and RNA templates. The pseudorotaxane formed to 30% for DNA and 10% for RNA even at 37 °C. The template with a mismatch sequence did not form pseudorotaxane with the cyclized ODN (Figure S9). Moreover the cyclized ODN and the template, which disassembled from the pseudorotaxane by heating at 80 °C, could reform the pseudorotaxane structure by heating at 50 °C (Figure S10). These results indicate that this pseudorotaxane is formed with the cyclized ODN reversibly by the slipping process and formation is temperature controlled.

In conclusion, we have established a novel method for pseudorotaxane formation that targets nucleic acids using a pair of reactive oligodeoxynucleotides. The reactions proceeded smoothly when a pair of ODNs hybridized on target nucleic acids simultaneously at the proper position. The resulting pseudorotaxanes were more stable than normal duplexes on denaturing polyacrylamide gels; however, the thermodynamic stability of the new duplexes was similar to that of standard duplexes. Interestingly, pseudorotaxane was formed with cyclized ODN reversibly via the slipping process. Since the method potentially enables the formation of pseudorotaxane with any single-stranded nucleic acids using only a pair of reactive ODNs, it represents a suitable method for a variety of applications in physiological conditions, such as new DNA nanotechnologies and antisense oligonucleotides. For example, *in situ* formation of pseudorotaxane with natural nucleic acids should expand the potential of DNA nanotechnologies, such as the development of DNA nanomachines suitable for a wider array of biological systems. We also expect that the molecular ring of pseudorotaxane will bind with mRNA tightly and strongly inhibit translation.

## ■ ASSOCIATED CONTENT

### Supporting Information

Experimental details, additional figures, and MALDI-TOF MS data. This material is available free of charge via the Internet at <http://pubs.acs.org>.

## ■ AUTHOR INFORMATION

### Corresponding Authors

h-abe@pharm.hokudai.ac.jp (H.A.)  
onizuka@tagen.tohoku.ac.jp (K.O.)

### Notes

The authors declare no competing financial interest.

## ■ ACKNOWLEDGMENTS

H.A. was financially supported by the Ministry of Education, Culture, Sports, Science, and Technology (MEXT), Precursory Research for Embryonic Science and Technology (PREST). K.O. was financially supported by the Special Postdoctoral Researcher Program of RIKEN. We are grateful for the support received from the Brain Science Institute (BSI) Research Resource Center for mass spectrum analysis.

## ■ REFERENCES

- (1) Balzani, V. V.; Credi, A.; Raymo, F. M.; Stoddart, J. F. *Angew. Chem., Int. Ed.* **2000**, *39*, 3348.
- (2) Collin, J. P.; Dietrich-Buchecker, C.; Gavina, P.; Jimenez-Molero, M. C.; Sauvage, J. P. *Acc. Chem. Res.* **2001**, *34*, 477.

- (3) Lewandowski, B.; De Bo, G.; Ward, J. W.; Pappmeyer, M.; Kuschel, S.; Aldegunde, M. J.; Gramlich, P. M.; Heckmann, D.; Goldup, S. M.; D'Souza, D. M.; Fernandes, A. E.; Leigh, D. A. *Science* **2013**, *339*, 189.
- (4) Thordarson, P.; Bijsterveld, E. J.; Rowan, A. E.; Nolte, R. J. *Nature* **2003**, *424*, 915.
- (5) Takashima, Y.; Osaki, M.; Ishimaru, Y.; Yamaguchi, H.; Harada, A. *Angew. Chem., Int. Ed.* **2011**, *50*, 7524.
- (6) Blanco, V.; Carlone, A.; Hanni, K. D.; Leigh, D. A.; Lewandowski, B. *Angew. Chem., Int. Ed.* **2012**, *51*, 5166.
- (7) van Dongen, S. F.; Clerx, J.; Norgaard, K.; Bloembergen, T. G.; Cornelissen, J. J.; Trakselis, M. A.; Nelson, S. W.; Benkovic, S. J.; Rowan, A. E.; Nolte, R. J. *Nat. Chem.* **2013**, *5*, 945.
- (8) Kumar, R.; El-Sagheer, A.; Tumpene, J.; Lincoln, P.; Wilhelmsson, L. M.; Brown, T. J. *Am. Chem. Soc.* **2007**, *129*, 6859.
- (9) Ackermand, D.; Schmidt, T. L.; Hannam, J. S.; Purohit, C. S.; Heckel, A.; Famulok, M. *Nat. Nanotechnol.* **2010**, *5*, 436.
- (10) Schmidt, T. L.; Heckel, A. *Nano Lett.* **2011**, *11*, 1739.
- (11) Lohmann, F.; Ackermand, D.; Famulok, M. *J. Am. Chem. Soc.* **2012**, *134*, 11884.
- (12) Sannohe, Y.; Sugiyama, H. *Bioorg. Med. Chem.* **2012**, *20*, 2030.
- (13) Ackermand, D.; Famulok, M. *Nucleic Acids Res.* **2013**, *41*, 4729.
- (14) Nilsson, M.; Malmgren, H.; Samiotaki, M.; Kwiatkowski, M.; Chowdhary, B. P.; Landegren, U. *Science* **1994**, *265*, 2085.
- (15) Escude, C.; Garestier, T.; Helene, C. *Proc. Natl. Acad. Sci. U.S.A.* **1999**, *96*, 10603.
- (16) Roulon, T.; Helene, C.; Escude, C. *Bioconjugate Chem.* **2002**, *13*, 1134.
- (17) Liu, Y.; Kuzuya, A.; Sha, R.; Guillaume, J.; Wang, R.; Canary, J. W.; Seeman, N. C. *J. Am. Chem. Soc.* **2008**, *130*, 10882.
- (18) Wang, S.; Kool, E. T. *Nucleic Acids Res.* **1994**, *22*, 2326.
- (19) Ryan, K.; Kool, E. T. *Chem. Biol.* **1998**, *5*, 59.
- (20) Fujimoto, K.; Matsuda, S.; Yoshimura, Y.; Ami, T.; Saito, I. *Chem. Commun.* **2007**, 2968.
- (21) Fujimoto, K.; Matsuda, S.; Ogawa, N.; Hayashi, M.; Saito, I. *Tetrahedron Lett.* **2000**, *41*, 6451.
- (22) Kole, R.; Krainer, A. R.; Altman, S. *Nat. Rev. Drug Discovery* **2012**, *11*, 125.
- (23) Abe, H.; Kondo, Y.; Jinmei, H.; Abe, N.; Furukawa, K.; Uchiyama, A.; Tsuneda, S.; Aikawa, K.; Matsumoto, I.; Ito, Y. *Bioconjugate Chem.* **2008**, *19*, 327.
- (24) Baskin, J. M.; Prescher, J. A.; Laughlin, S. T.; Agard, N. J.; Chang, P. V.; Miller, I. A.; Lo, A.; Codelli, J. A.; Bertozzi, C. R. *Proc. Natl. Acad. Sci. U.S.A.* **2007**, *104*, 16793.
- (25) Jewett, J. C.; Sletten, E. M.; Bertozzi, C. R. *J. Am. Chem. Soc.* **2010**, *132*, 3688.
- (26) Shelbourne, M.; Chen, X.; Brown, T.; El-Sagheer, A. H. *Chem. Commun.* **2011**, *47*, 6257.
- (27) Leslie, A. G. W.; Arnott, S.; Chandrasekaran, R.; Ratliff, R. L. *J. Mol. Biol.* **1980**, *143*, 49.
- (28) Asakawa, M.; Ashton, P. R.; Ballardini, R.; Balzani, V.; Belohradsky, M.; Gandolfi, M. T.; Kocian, O.; Prodi, L.; Raymo, F. M.; Stoddart, J. F.; Venturi, M. *J. Am. Chem. Soc.* **1997**, *119*, 302.